JOURNAL OF
Materials
CHEMISTRY
Communication

Syntheses of nano-sized cubic phase early transition metal carbides from metal chlorides and n-butyllithium

Yu-Hsu Chang, Ching-Wen Chiu, Yung-Chun Chen, Chia-Chen Wu, Chih-Pin Tsai, Je-Lin Wang and Hsin-Tien Chiu*

Department of Applied Chemistry, National Chiao Tung University, Hsinchu, Taiwan, 30050, R. O. C. E-mail: htchiu@cc.nctu.edu.tw; Tel: 886-3-5131524; Fax: 886-3-5723764

Received 23rd April 2002, Accepted 7th May 2002
First published as an Advance Article on the web 29th May 2002

Nano-sized early transition metal carbides, including TiC, ZrC, HfC, V_4C_3, NbC and TaC, were synthesized from colloidal precursors generated by reducing the metal chlorides, $TiCl_4$, $ZrCl_4$, $HfCl_4$, VCl_3, $NbCl_5$, and $TaCl_5$, respectively, with n-C_4H_9Li in hexane. The colloids were formed from the reduction of the metal centers, which then nucleated into nano-scaled metal clusters. The major byproducts were LiCl, C_4H_{10}, and C_4H_8, indicating that the butyl groups probably underwent β-hydrogen elimination and reductive elimination. This suggests that C–C bond activation of the butyl groups was in operation, leaving residual carbon atoms in the metal colloids. The colloids were further heated at 873–1273 K to crystallize into cubic phase TiC, ZrC, HfC, V_4C_3, NbC and TaC nanoparticles.

Early transition metal carbides have many potential applications due to their special properties, such as extremely high melting points (2000–4000 K), excellent high-temperature strength and good corrosion resistance.[1–3] For example, they can be used in rocket nozzles and drill bits. Many transition metal carbides also show interesting catalytic behavior,[2] such as hydrogenation, hydrogenolysis, isomerization, hydrodesulfurization and hydrodenitrogenation of hydrocarbons. Transition metal carbides have been explored for their potential applications as the diffusion barrier in electronic devices, too.[4] Many routes to transition metal carbides are known. These include mechanical milling,[5–7] solid-state metathesis reactions,[8,9] reduction–carburization routes[10–13] under high temperature or high pressure, and polymeric precursor routes using metal alkoxides to react with other organic compounds.[14–17] Recently, high surface area Mo_2C and WC nanoparticles were synthesized by alkalide reduction.[18] Here we present a new method to prepare nano-sized metal carbides, derived from basic organometallic reactions, β-hydrogen elimination and reductive elimination. It is well known that alkyl groups with β-hydrogens do not form stable transition metal alkyl complexes. The reason is that the β-hydrogen atoms of the alkyl groups can interact with the metal center to undergo the low-energy β-hydrogen elimination reaction pathway.[19] Reductive elimination is another fundamental organometallic reaction process.[20,21] In this reaction, two ligands bound to the metal center are coupled and removed as the formal oxidation state of the metal center is reduced by two. Many simple homolytic organometallic compounds were not stable enough to be isolated probably due to the presence of these undesired reaction pathways. We take the advantage of this unstable nature between alkyl groups with β-hydrogen atoms and transition metals to prepare nano-sized transition metal carbides under relatively mild conditions.

Generally, early transition metal chlorides MCl_x (M: Ti, Zr, Hf, V, Nb, Ta) were reacted with ^{n}BuLi, n-butyllithium, in hexane to form black colloids. The colloids were separated and annealed at high temperatures to increase their stability and crystallinity.[22] This process also separated the byproduct LiCl from the solid by sublimation. General reaction conditions are summarized in Table 1. Other volatile products were collected and identified by using NMR (nuclear magnetic resonance), FT-IR (Fourier transform infrared) spectroscopy and GC-MS (gas-chromatography–mass spectrometry). Below, several examples are described in detail.

After the colloid formed from the reaction between $TiCl_4$ and ^{n}BuLi was annealed at 1273 K under low pressure for 2 h, nano-sized particles were collected. In Fig. 1a, TEM (transmission electron microscopy) analysis reveals that the particles are less than 15 nm in diameter. The ED (electron diffraction) study shows a ring pattern, indicating that the powder is polycrystalline. Analysis of the pattern suggests that the material is cubic with an estimated lattice parameter $a = 0.43$ nm. The value is close to the literature data of TiC,[23] $a = 0.43274$ nm. The XRD (X-ray diffraction) pattern is shown in Fig. 2a and peaks are assigned to the (111), (200), (220), (311) and (222) reflections of a face-centered cubic structure. The lattice parameter a is calculated to be 0.4321 nm which is close to the reported value and the data from the ED study. The broadening of the peaks is due to the small crystal size. The

Table 1 Summary of the reactions between metal chlorides and n-butyllithium

MX_x	^{n}BuLi (equiv.)	Reaction temp./K	Reaction time/h	Annealing temp./K	Annealing time/h	Size by TEM/nm	Size by XRD/nm	a_{obs} by XRD/nm	a_{lit} by XRD/nm	Phase of powders
$TiCl_4$	4	273	0.5	1073–1273	1–2	10–20	10	0.4321	0.43274	Cubic TiC
$ZrCl_4$	4	273	1.0	973–1273	2–12	—	7	0.4688	0.4693	Cubic ZrC
$HfCl_4$	4	343	12	1073–1273	2–12	10–50	[a]	[a]	0.4637	Cubic HfC
VCl_3	3	273	12	873–1273	6–12	10–30	9	0.4157	0.416	Cubic V_4C_3
$NbCl_5$	5	273	12	873–1273	6–12	10–20	9	0.4470	0.4469	Cubic NbC
$TaCl_5$	5	273	12	973–1273	6–12	—	7	0.4449	0.4454	Cubic TaC

[a] The signal width is too broad to be estimated accurately.

DOI: 10.1039/b203927c

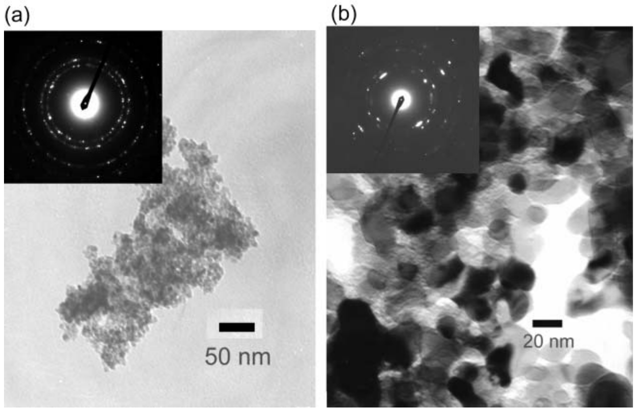

Fig. 1 TEM and ED images of (a) TiC nanoparticles annealed at 1273 K, and (b) V_4C_3 nanoparticles annealed at 1073 K.

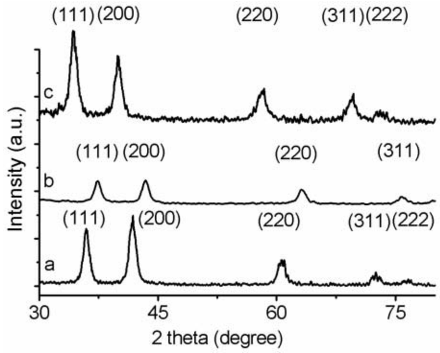

Fig. 2 XRD patterns of (a) TiC nanoparticles annealed at 1273 K, (b) V_4C_3 nanoparticles annealed at 1073 K and (c) NbC nanoparticles annealed at 1273 K.

average crystal size estimated from the Scherrer equation[24] is 10 nm. The XPS (X-ray photoelectron spectra) showed that the binding energy of the C 1s electron was at 282.1 eV, while the binding energies of the Ti $2p_{3/2}$ and Ti $2p_{1/2}$ electrons were at 455.1 eV and 461.5 eV, respectively. This result agrees with the literature report of titanium carbide.[25] In addition, there is a minor signal at 284.6 eV which is attributable to the presence of some graphitic carbon. The XPS study also showed a trace amount of oxygen in the sample, which is due to the oxophilic nature of the early transition metals. Furthermore, the surface area was estimated by the BET method.[26] For the TiC prepared at 1273 K, the surface area is 60 $m^2\ g^{-1}$ by assuming that the particles are spherical, the mean diameter is estimated to be 18 nm. This observation is in good agreement with the TEM image in Fig. 1a. The powders obtained below 873 K were pyrophoric, probably the size is too small to be stable in air. Analyses of the reaction byproducts by GC-MS and FT-IR revealed the presence of C_4H_{10} and C_4H_8 as the major volatile products. Traces of other hydrocarbons were also detected but were not separated further. Formation of butane and but-1-ene at room temperature was also observed by NMR for the reaction of $TiCl_4$ and ^nBuLi in a sealed NMR tube. LiCl was sublimed from the colloids and identified by XRD.

A TEM image of V_4C_3 nanoparticles of 10–30 nm diameter is shown in Fig. 1b. They were precipitated from the reaction employing VCl_3 and ^nBuLi and annealed at 1073 K after separation. Analysis of the ED data indicates that the ring pattern corresponds to a polycrystalline solid with a cubic structure and a lattice parameter $a = 0.42$ nm. The value is close to the reported data of V_4C_3,[23] $a = 0.416$ nm. The XRD pattern (Fig. 2b) of the product shows a reflection pattern of V_4C_3 with the lattice parameter $a = 0.4157$ nm. The estimated crystal size is 9 nm using the Scherrer equation. NbC nanoparticles were precipitated from a reaction employing $NbCl_5$ and ^nBuLi, and annealed at 1273 K. The TEM image showed that the size was 10–20 nm in diameter. The ring pattern of the ED corresponded to a polycrystalline solid with a cubic structure and a lattice parameter $a = 0.45$ nm. The value is close to the reported data of NbC, $a = 0.4469$ nm.[23] The XRD pattern (Fig. 2c) of the product shows a reflection pattern of NbC with the lattice parameter $a = 0.4470$ nm. Using the Scherrer equation, the crystal size is estimated to be 9 nm.

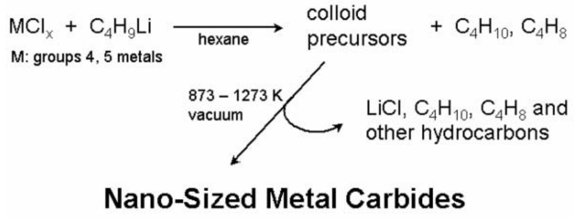

Scheme 1

The general reaction pathway is summarized in Scheme 1. Based on the reaction byproducts observed for the formation of the TiC nanoparticles and the well-studied organometallic reactions, we propose that the process consists of the following reaction steps. One of the steps is the metathetic reaction between the M–Cl bond and the Bu–Li bond. The step probably alkylated the metal center to form metal–carbon bonds and produced LiCl. Next, with the butyl ligands attached to the metal center, the β-hydrogen elimination[19] pathway provides a low-energy route to form butene and a metal–hydride intermediate. The butyl groups may couple to the hydride to undergo a reductive elimination process also,[20,21] which generates butane and a reduced metal center. Radical pathways are less likely because the formation of C_8H_{18} was not observed. The reduced metal centers nucleate and coagulate into colloids. These colloids were highly air-sensitive and difficult to manipulate. Based on the observation of the evolution of hydrocarbon byproducts, such as butane and butene, from the colloids after the heat treatment, we conclude that residual hydrocarbon groups might still be in the isolated colloids. The colloids might contain LiCl in a separated solid phase. However, we cannot rule out the possibility that the colloids contained mixed metal complexes $LiRMCl_x$. After they are heat-treated, some C–C bonds of the hydrocarbon ligands are activated. This produces the carbidic carbon atoms in the solid state. As active sites are easily accessible on the colloid's surface, polymerization of the hydrocarbon fragments is also possible. This may produce the graphitic carbons found in the particles.

This study has shown that by proper selection of reaction precursors, transition metal carbides can be prepared at temperatures significantly lower than those employed in the traditional methods. The origin of this improvement is probably due to the formation of metal–alkyl bonds at low temperatures in solution. The β-hydrogen elimination and the reductive elimination of the metal–alkyl linkage provide low-energy pathways to form reactive metal colloids, which activates C–C bonds and allows uniform mixing of the elements at the atomic level. This lowers the subsequent energy barriers for metal carbide formation. Detailed studies are in progress.

Acknowledgement

The authors thank the National Science Council of Taiwan, Republic of China (NSC-89-2113-M-009-013) and Chinese Petroleum Corporation (88-CPC-M-009-002) for financial support.

Notes and references

1 L. E. Toth, in *Transition Metal Carbides and Nitrides*, Academic Press, New York, 1971.

2 S. T. Oyama, in *The Chemistry of Transition Metal Carbides and Nitrides*, Blackie Academic and Professional, Glasgow, 1996.

3 H. O. Pierson, in *Handbook of Refractory Carbides and Nitrides*, Noyes Publications, Westwood, 1996.

4 H.-Y. Tsai, S.-C. Sun and S.-J. Wang, *J. Electrochem. Soc.*, 2000, **147**, 2766.

5 N. J. Welham and D. J. Llewellyn, *J. Eur. Ceram. Soc.*, 1999, **19**, 2833.

6 M. S. El-Eskandarany, *Metall. Mater. Trans. A*, 1996, **27**, 2374.

7 N. J. Welham, *J. Mater. Sci.*, 1999, **34**, 21.

8 A. M. Nartowski, I. P. Parkin, A. J. Craven and M. MacKenzie, *Adv. Mater.*, 1998, **10**, 805.

9 A. M. Nartowski, I. P. Parkin, M. MacKenzie, A. J. Craven and I. MacLeod, *J. Mater. Chem.*, 1999, **9**, 1275.

10 J. Q. Hu, Q. Y. Lu, K. B. Tang, B. Deng, R. Jiang, Y. T. Qian, G. E. Zhou and L. Yang, *Chem. Lett.*, 2000, **5**, 474.

11 R. Kapoor and S. T. Oyama, *J. Solid State Chem.*, 1995, **120**, 320.

12 G.-Y. Xu, Y. Huang, J.-B. Li and Z.-P. Xie, *J. Mater. Sci. Lett.*, 1999, **18**, 827.

13 H. Preiss, B. Meyer and C. Olschewski, *J. Mater. Sci.*, 1998, **33**, 713.

14 Z. Jiang and W. E. Rhine, *Chem. Mater.*, 1991, **3**, 1132.

15 S. Dutremez, P. Gerbier, C. Guerin, B. Henner and P. Merle, *Adv. Mater.*, 1998, **10**, 465.

16 Y. Kurokawa, S. Kobayashi, M. Suzuki, M. Shimazaki and M. Takahashi, *J. Mater. Res.*, 1998, **13**, 760.

17 V. L. S. Teixeira da Silva, E. I. Ko, M. Schmal and S. T. Oyama, *Chem. Mater.*, 1995, **7**, 179.

18 J. A. Nelson and M. J. Wagner, *Chem. Mater.*, 2002, **14**, 1639.

19 G. M. Whitesides, J. F. Gaasch and E. R. Stedronsky, *J. Am. Chem. Soc.*, 1972, **94**, 5258.

20 J. M. Brown and N. A. Cooley, *Chem. Rev.*, 1988, **88**, 1031.

21 A. C. Balazs, K. H. Johnson and G. M. Whitesides, *Inorg. Chem.*, 1982, **21**, 2162.

22 All procedures were carried out using standard airless manipulation techniques. MCl_x (*ca.* 50 mmol) was allowed to react with a stoichiometric amount of ^{n}BuLi slowly in hexane (50 mL) at 273 K. After mixing, air-sensitive black precipitates were formed. The colloids were separated, dried under vacuum, and processed further. LiCl and other volatile byproducts were removed by vacuum sublimation at 873 K. Then, the samples were annealed at 873–1273 K for 1–10 h under vacuum and then cooled to room temperature. The reaction conditions are summarized in Table 1. XRD studies were carried out using a MAC MXP-3 diffractometer with Cu Kα radiation. TEM and ED data collection was accomplished on a JEOL JEM-2000FX instrument operating at 200 KeV. The XPS measurements were carried out using a Perkin-Elmer PHI-1600 spectrometer with Mg Kα (1253.6 eV) radiation. The volatile products were analyzed by a Varian Unity-300 NMR spectrometer, a Perkin-Elmer System 2000 FT-IR spectrometer and a VG Biotech trio-2000 GC-MS spectrometer.

23 Powder diffraction file cards 32-1383 (TiC), 35-0784 (ZrC), 39-1491 (HfC), 1-1159 (V_4C_3), 38-1364 (NbC) and 35-0801 (TaC). JCPDS: International Center for Diffraction Data, 1601 Park Lane, Swarthmore, PA 19081.

24 H. P. Klug and L. E. Alexander, in *X-Ray Diffraction Procedure for Polycrystalline and Amorphous Materials*, 2nd edn., John Wiley & Sons, New York, 1974.

25 H. Ihara, Y. Kumashiro, A. Itoh and K. Maeda, *Jpn. J. Appl. Phys.*, 1973, **12**, 1462.

26 T. Allen, in *Particle Size Measurement*, Chapman and Hall, London, 1990.